Published in final edited form as:
J Neuroimmune Pharmacol. 2010 December ; 5(4): 592–601. doi:10.1007/s11481-010-9198-7.

Nanoformulated Antiretroviral Combinations Extend Drug Release and Antiretroviral Responses in HIV-1 Infected Macrophages: Implications for NeuroAIDS Therapeutics

Ari S. Nowacek, BS[1], **JoEllyn McMillan, PhD**[1], **Reagan Miller, PhD**[2], **Alec Anderson, BS**[1], **Barrett Rabinow, PhD**[2], and **Howard E. Gendelman, MD**[1]

[1]Department of Pharmacology and Experimental Neuroscience, University of Nebraska Medical Center, Omaha, NE 68198-5880 USA

[2]Baxter Healthcare Corporation, Round Lake, IL 60073

Abstract

We posit that improvements in pharmacokinetics and biodistributions of antiretroviral therapies (ART) for human immunodeficiency virus-type one infected people can be achieved through developments in nanoformulations. To this end, we manufactured nanoparticles of atazanavir, efavirenz, and ritonavir (termed nanoART) and treated human monocyte-derived macrophages (MDM) in combination therapies. This resulted in improved drug uptake, release and antiretroviral efficacy over monotherapy. MDM rapidly, within minutes, ingested nanoART combinations, at equal or similar rates, as individual formulations. Combination nanoART ingested by MDM facilitated drug release from 15 to > 20 days. These findings are noteworthy as a nanoART cell-mediated drug delivery provides a means to deliver therapeutics to viral sanctuaries, such as the central nervous system during progressive human immunodeficiency virus-type one infection. The work brings us yet another step closer to realizing the utility of nanoART for virus-infected people.

Keywords

antiretroviral therapy; nanoparticles; macrophages; drug delivery; HIV; nanomedicine

Introduction

Antiretroviral medications are effective at inhibiting viral replication or interrupting the viral life cycle. As a result, antiretroviral therapy (ART) has reduced morbidity and mortality inhuman immunodeficiency virus type one (HIV-1) infected people. However, a major limitation of ART is the need for lifelong daily treatment(Garvie et al., 2009; Royal et al., 2009). Suboptimal adherence to daily therapy increases the risk of treatment failure and development of viral resistance and commonly results in accelerated progression of disease (Paterson et al., 2000; Mascolini et al., 2008; Danel et al., 2009; Metzner et al., 2009). Factors such as concomitant drug abuse, psychiatric and mental disorders, and drug side effects often lead to sporadic adherence(Baum et al., 2009; Meade et al., 2009). In this

*Corresponding author: Howard E. Gendelman, M.D., Department of Pharmacology and Experimental Neuroscience, 985880 Nebraska Medical Center, Omaha, NE 68198-5880 USA, hegendel@unmc.edu, Phone: 402-559-8920, Fax: 402-559-3744.

Financial & competing interests disclosures
The work was supported by National Institutes of Health grants 2R01 NS034239, 2R37 NS36126, P01 NS31492, P20RR 15635, P01 MH64570, and P01 NS43985 (to H.E.G.) and from a research grant from Baxter Healthcare.

regard, providers are commonly reluctant to prescribe ART to those patients who are poorly compliant because of concerns about the promotion of viral resistance(Bruce et al., 2006a; Bruce et al., 2006b). Complicating matters further are the common cognitive and motor disorders that result as a consequence of HIV-1 infection(Epstein and Gendelman, 1993). These risk factors, taken together, often result in poor treatment outcomes(Murri et al., 2006). Means to overcome such concerns are being developed in our laboratories. Indeed, slow release nanoformulated ART, termed nanoART, could travel to sites of infection and slowly release drug(s) with limited tissue toxicities(Kabanov and Gendelman, 2007; Nowacek and Gendelman, 2009). Such a drug delivery system, if realized, could revolutionize ART and improve outcomes, particularly those within the central nervous system (CNS).

To this end, we synthesized nanoART that are carried within circulating monocyte-macrophages, delivered to virus-target tissues, and released in time periods measured in weeks(Dou et al., 2006; Dou et al., 2007; Dou et al., 2009; Nowacek et al., 2009b). Unfortunately, there are a number of obstacles that need to be overcome before nanoART can be moved from the bench to the bedside. These include optimizing cellular uptake, preventing drug metabolism and degradation, and reducing untoward side effects. In an effort to overcome these obstacles, we used homogenization and sonication techniques to process poorly water-soluble drugs for nanoART manufacture. Previously, we demonstrated that cellular handling of antiretroviral drugs could be accomplished by altering the physical properties of nanoparticles (NP) (Nowacek et al., 2009b). NanoART-treated monocyte-derived macrophages (MDM)could protect against HIV-1infection for up to 15 days(Nowacek et al., 2009b). However, these studies were performed using single drug formulations. We posit that by using nanoART combination therapy we can extend the drug release and improve viral inhibition. To accomplish this, we tested nanoformulations of atazanavir (ATV), ritonavir (RTV), and efavirenz (EFV)in combination in MDM cultures. Our results show that MDM can simultaneously uptake three nanoART formulations without a reduction in total drug uptake. In addition, we extended the time of drug release and improved antiretroviral efficacy.

These data strongly suggest that the effects of nanoART could be enhanced by combination therapy. All together, the data implies that cell-mediated nanoART delivery can control HIV-1 infection. The use of such technology could both impact the administration of ART and help to eliminate virus from its sanctuaries, such as the CNS, where migration of MDM is a major mechanism for viral dissemination(Kraft-Terry et al., 2009).

Materials and Methods

Preparation and characterization of nanoART

NanoART of ATV and RTV were prepared by high-pressure homogenization using an Avestin C-5 homogenizer (Avestin, Inc., Ottawa, Ontario, Canada) as previously described, (Nowacek et al., 2009b). Surfactants used to coat the drug crystals included a block copolymer of ethylene oxide and propylene oxide, Poloxamer 188 (P-188)(Spectrum Chemicals, Gardena, CA), 1,2-distearoyl-phosphatidyl-ethanolamine-methyl-poly-ethylene-glycol (DSPE-mPEG$_{2000}$) (Genzyme, Cambridge, MA), and 1-oleoyl-2-[6-[(7-nitro-2-1,3-benzoxadiazol-4-yl)amino]hexanoyl]-3-trimethylammonium propane (DOTAP) (Genzyme). To coat the nanosized drug crystals, each surfactant was made up (weight/weight %) of P-188 (0.5%), mPEG$_{2000}$-DSPE (0.2%), and DOTAP (0.1%). The nanosuspensions were formulated at a slightly alkaline pH of 7.8 using either 10 mM sodium phosphate or 10 mM HEPES as a buffer. Tonicity was adjusted with glycerin (2.25%) or sucrose (9.25%). Free base drug was added to the surfactant solution to make a concentration of approximately 2% [weight to volume ratio (%)]. Lissamine rhodamine B 1,2-dihexadecanoyl-sn-glycero-3-

phosphoethanolamine, triethylammonium salt (Ex 560 nm: Em 580 nm) (Invitrogen, Carlsbad, CA) was used to label ATV-H1045, which appeared as red fluorescence. Vybrant DiO cell-labeling solution (Ex 484 nm: Em 501 nm, Invitrogen) was used to label RTV-H1025, which appeared as green fluorescence. In order to synthesize nanoART, a suspension was prepared by adding crystalline drug to a surfactant solution and mixing for 4 – 7 min using an Ultra-Turrax T-18 (IKA® Works Inc., Wilmington, NC) rotor-stator mixer to reduce initial particle size. The suspension was homogenized at 20,000 psi for approximately 30 passes or until desired particle size was reached.

For preparation of EFV-P1044, drug free base was suspended within nanosized droplets of poly(lactic-co-glycolic acid) (PLGA, ratio 50:50 of lactide to glycolide)(Sigma-Aldrich, St. Louis, MO) and cetyltrimethyl ammonium bromide (CTAB) (Sigma-Aldrich). EFV (1.25 g), PLGA (6.0 g), and CTAB (0.50 g) were dissolved in dichloromethane (50 mL) and added to a 1% poly(vinyl) alcohol solution (500 mL). Particle size was achieved by sonicating at 50% amplitude for 10 min using a 400/600 Watt sonicator with ¾ inch high gain probe. Stirring overnight to evaporate the dichloromethane hardened particles. The suspension was then centrifuged, washed with distilled/deionized water, and decanted twice. The particles were suspended in 10% mannitol before being frozen or lyophilized for storage. Vybrant DiD cell-labeling solution (Ex 644 nm: Em 665 nm) (Invitrogen) was used to label EFV-P1044, which appeared as far-red fluorescence. For all nanosuspensions, particle size was measured using a HORIBA LA 920 light scattering instrument (HORIBA Instruments Inc., Irvine, CA). Zeta potential was measured by diluting 0.1 ml of the suspension into 9.9 ml of 10 mM HEPES, pH 7.4 on a Malvern Zetasizer Nano series instrument (Malvern Instruments Inc., Westborough, MA). Final drug content of the formulations was determined by reversed phase high performance liquid chromatography (HPLC) (data not shown).

Human monocyte isolation and cultivation

Human monocytes were obtained by leukapheresis from HIV-1,2 and hepatitis seronegative donors and were purified by counter-current centrifugal elutriation(Gendelman et al., 1988). As previously described(Nowacek et al., 2009b), monocytes were cultured at a concentration of 1×10^6 cells/ml in the presence of recombinant human macrophage colony stimulating factor(a generous gift of Wyeth Inc., Cambridge, MA) to induce differentiation to macrophages.

NanoART uptake and release

MDM (2×10^6 cells per well) were cultured with nanoART at a concentration of 100 μM for each nanoformulation alone or when used in combination. Therefore, cells exposed to a combination of the nanoformulations were treated with a total of 300 μM of drug (100 μM of each) within the medium. Uptake of nanoART was assessed without medium change for 24 h with cell collection occurring at indicated times points. Release of drug(s) into surrounding medium from nanoART treated cells was also evaluated. After an initial 12 h exposure to nanoART, MDM were washed 3 times with phosphate buffered saline (PBS), given drug free medium, and underwent a half media exchange every other day for 20 days. Adherent MDM and corresponding medium samples were collected every other day, stored at −80° C, and processed for HPLC. Prepared samples were assessed by HPLC using triplicate 20 μl injections onto a YMC Octyl C8 column (Waters Inc., Milford, MA) with a C8 guard cartridge. Mobile phase consisting of 48% acetonitrile / 52% 25mM KH_2PO_4, pH 4.15, was pumped at 0.4 ml/min with UV/V is detection at 272 nm. For all antiretroviral drugs, quantitations were determined by comparison to a standard curve of each free drug (0.025–100 μg/ml) prepared in methanol.

Electron microscopy

Samples were fixed by 3% glutaraldehyde in 0.1 M phosphate buffer (pH 7.4) and further fixed in 1% osmium tetroxide in 0.1 M phosphate buffer (pH 7.4) for 1 h. Samples were dehydrated in a graduated ethanol series and embedded in Epon 812 (Electron Microscopic Sciences, Fort Washington, PA) for scanning electron microscopy. Thin sections (80 nm) were stained with uranyl acetate and lead citrate and observed under a transmission electron microscope (Hitachi H7500-I) (Hitachi High Technologies America Inc., Schaumburg, IL) for transmission electron microscopy.

Confocal microscopy

NPs were labeled with fluorescent phospholipids as described above. Unlabeled MDM were then treated with fluorescent NPs for 4 h, washed 3 times with PBS, and were imaged using a Nikon TE2000-U (Nikon Instruments Inc., Melville, NY) with swept-field confocal microscope, 488 nm (green), 568 nm (red), and 633 nm (color) laser excitations, and a 60x objective.

Antiretroviral activities of nanoART

MDM were treated with nanoART for 12 h, washed to remove excess drug, and infected with HIV-1_{ADA} at a multiplicity of infection (MOI) of 0.01 infectious viral particles/cell (Gendelman et al., 1988)on days 5, 10, 15, and 20 after treatment. Following viral infection, cells were cultured for ten days with half media exchanges every other day. Culture fluids were collected 10 days after infection for measurements of progeny virion production as assayed by reverse transcriptase (RT) activity(Kalter et al., 1991). Parallel analyses for expression of HIV-1 p24 antigen in infected cells were performed by immunostaining on the same day as culture fluid sampling.

RT assay

In a 96-well plate, media samples (10 μl) were mixed with 10 μl of a solution containing 100 mM Tris-HCl (pH 7.9), 300 mM KCl, 10 mM DTT, 0.1% nonyl phenoxylpoly-ethoxylethanol-40 (NP-40), and water. The reaction mixture was incubated at 37°C for 15 min; and 25 μl of a solution containing 50 mM Tris-HCl (pH 7.9), 150 mM KCl, 5 mM DTT, 15 mM $MgCl_2$, 0.05% NP-40, 10 μg/ml poly(A), 0.250 U/ml oligo $d(T)_{12–18}$, and 10 μCi/ml ^{3}H-TTP was added to each well. Plates were incubated at 37°C for 18 h. Following incubation, 50 μl of cold 10% trichloroacetic acid (TCA) was added to each well. The wells were harvested onto glass fiber filters, and the filters were assessed for ^{3}H-TTP incorporation by β-scintillation spectroscopy using a TopCount NXT (PerkinElmer Inc., Waltham, MA) (Kalter et al., 1991).

Immunohistochemistry

Cells were fixed with 4% phosphate-buffered paraformaldehyde 10 days after HIV-1 infection. Mouse monoclonal antibodies to HIV-1 p24 (1:10, Dako, Carpinteria, CA) were used to visualize p24. Images of cells were acquired using a Nikon TE300 (Nikon, San Diego, CA) and a 40x objective.

Cytotoxicity

To determine any potential toxic effects of NP on cells, MDM were treated with NP for 12 h at the same concentrations as used in all other studies, and cytotoxicity assessed 24 h later using a mitochondrial 3-(4,5-dimethylthiazol-2-yl)-2,5-diphenyltetrazolium bromide (MTT)assay (Mosmann, 1983).

Statistical analyses

All data analyses were carried out using Prism (GraphPad Software, Inc., La Jolla, CA). Significant differences in drug levels in uptake and release studies were determined by two-way ANOVA followed by Bonferroni's Multiple Comparison Test. Significant differences in RT activity were determined by one-way ANOVA followed by Bonferroni's Multiple Comparison Test. A p-value of ≤ 0.05 was considered significant.

Results

Manufacture and characterization of nanoART

NanoART were manufactured as nanosized drug crystals prepared from free-base drug and coated with phospholipid surfactants (ATV and RTV)or drug dissolved in a PLGA copolymer solution (EFV). The physical properties of nanosuspensions were similar in both size and charge (Table 1). The zeta potentials of all three nanoART were positive and ranged from +7.4 mV for EFV-P1044 to +15.5 mV for RTV-H1025. The average size ranged from 300 nm for EFV-P1044 to 645 nm for ATV-H1045. NanoART suspensions showed distinctive morphologies based upon drug and manufacturing method. ATV-H1045 particles were polygonal in shape with distinct smooth-surfaces (Fig. 1A). EFV-P1044 particles were spherical with distinct and smooth-surfaces (Fig. 1B). RTV-H1025 particles were rod shaped with sharp and geometrically varied edges (Fig. 1C). Transmission electron microscopy of MDM co-cultured with all three nanoART in combination demonstrated co-localization to the cytoplasm with retention of each nanoART's structural integrity. Each nanoART within the cell is readily identifiable by its distinctive shape (Fig. 1D, colored outlines). Transmission electron microscopy of untreated MDM demonstrated no such structures (Fig. 1E).

NP uptake and antiretroviral drug release

In addition to transmission electron microscopy, confocal microscopy was also used to visualize uptake of the combination of nanoART into MDM. Cells were treated with fluorescently labeled ATV-H1045, EFV-P1044, and RTV-H1025 for 4h and imaged by confocal microscopy. All three nanoART formulations were taken up by the MDM and co-localized in the cytoplasm as indicated by white in the overlay image (Fig. 2). A z-stack of the same image shows nanoART localized to the cytoplasm of the cells (Supplemental 1).

To quantify MDM uptake of RTV, ATV and EFV in a combination nanoART treatment, cells were treated alone or in combination with 100 μM of each formulation over a 24 hr period. Cellular content of the drug was analyzed by HPLC. There were no significant differences in either rate of uptake or maximum amount of drug accumulated when nanoART were used alone or in combination (Fig. 3). In all cases, nanoART were taken up rapidly by MDM (< 30 min), and 95% of maximum uptake was achieved by 8 hrs. The maximum amount of uptake was 35 $\mu g/10^6$ cells for ATZ-H1045, 2 $\mu g/10^6$ cells for EFV-P1044, and 50 $\mu g/10^6$ cells for RTV-H1025 for both monotherapy and combination therapy (Fig. 3). Treatment regimens, both single and combination, did not result in any observed toxicity as determined by MTT assay (data not shown).

For release studies, the culture medium was replaced at 12 h with fresh medium without nanoART; and drug release into the medium was determined up to 20 days by HPLC. In both medium and cells, there was a significant ($p< 0.05$) difference in the release of drug between a nanoART formulation used alone or in combination. Drug retention within MDM was significantly ($p<0.05$)greater as early as day 5 post nanoART treatment for both ATV and EFV when used in combination compared to when used alone (Fig. 3). Drug concentrations within MDM were significantly ($p<0.05$) greater for all combined ART

treatments 15 days after drug removal and remained so for up to 20 days when compared to individual nanoART treatments (Fig. 3). In the case of EFV-P1044, no drug was detectable in MDM 20 days after treatment when cells were loaded with the nanoformulation alone; however, detectable levels of EFV were observed in the cells treated with the nanoART combo (Fig. 3). In the media, drug was still present at day 20 for all treatments (Fig. 3). However, drug levels within the medium were 1.5- to 2-fold higher when nanoART were used in combination compared to nanoART used individually (Fig. 3).

Antiretroviral efficacy of combination and individual nanoART therapies

The antiretroviral efficacy of the nanoART combination treatment was determined in MDM. Cells were treated with 100 μM ATV-H1045, 100 μM RTV-H1025 and 100 μM EFV-P1044 alone or in combination for 12 h. At this time, the drug(s) was/were removed and medium replaced with fresh medium without drug. At 1, 5, 10, 15 and 20 days after drug removal, cells were challenged with HIV-1_{ADA} at an MOI of 0.01 infectious virus particles per cell. RT activity and HIV-1 p24 antigen were assayed 10 days after viral challenge. RT activity was not detectable in any of the treatment groups through challenge day 15. When cells were challenged with infection on day 20 after drug removal, RT activity was reduced significantly ($p < 0.001$) by approximately 50% in cells treated with each nanoART alone as compared to cells given no drug (Fig. 4). Of importance, RT activity in cells treated with nanoART in combination was reduced nearly to levels observed in non-infected cells and was significantly ($p < 0.001$) lower than infected cells or cells treated with individual nanoARTs(Fig. 4). These results were confirmed by analysis of expression of HIV-1 p24 antigen (Fig. 5). In cells infected on challenge day 20, complete suppression of p24 antigen expression was observed in those cells treated with the combination nanoART, but there was only an approximate 50% reduction in cells treated with individual nanoART (Fig. 5). These results closely paralleled those seen for RT activity.

Discussion

Finding ways to effectively control HIV-1 infection remains a singular goal for ART. While current antiretroviral drugs reduce morbidity and mortality associated with viral infection, there are limitations that prevent ART from eradicating the virus in infected people. Indeed, a combination of drug-related biochemical, physiological, as well as human factors, continue to lead to treatment failure in a proportion of patients (Fellay et al., 2001; Hawkins, 2006). Notable is the formation of viral sanctuaries, such as the CNS, where ART compounds are unable to access and virus is allowed to replicate albeit at limited levels (Best et al., 2009; Varatharajan and Thomas, 2009). *First,* NanoART provides an important means to overcome this and other limitations for CNS drug delivery. In this report, we show that nanoART can be manufactured and optimized in laboratory models of HIV infection. *Second*, combinations of nanoART can improve antiretroviral efficacy without cytotoxicity. Viral breakthrough was seen 20 days after monotherapy for each drug while combination therapy still provided total viral inhibition at 20 days. The improvement in antiretroviral activities with combination therapy could potentially be due to the presence of more drugs and to having drugs with different mechanisms of action. *Third*, the particles were located within the same sub-cellular compartments. Interestingly, there was no reduction in the absolute amount of each drug taken up when cells were treated with combo nanoART compared to when each was used alone. *Fourth*, this work serves to bridge animal studies being developed to assess safety and efficacy with the final goal being human clinical trials. The fact that MDM are able to take up all three nanoART formulations simultaneously provides an important step in this direction. Also, that multiple nanoART can be loaded simultaneously and that uptake is not competitive among formulations supports its utility in an infected human host.

The cell-based delivery system developed in the current report is based on monocyte-macrophage function and viral dissemination in an infected human host. One focus of such infection is the brain. Indeed, HIV infection of the brain can result in both functional and cognitive deficits, a condition known as HIV-1 associated neurocognitive disorder (HAND) (Gray et al., 2001). Some form of neurological dysfunction is displayed in nearly half of people infected with HIV; this makes HAND a not infrequent cause of dementia worldwide (Valcour and Paul, 2006; Ellis et al., 2007; Varatharajan and Thomas, 2009). This is primarily due to the inability of ART medications to effectively cross the blood-brain barrier (BBB) or to persist within the parenchyma upon entering the CNS (reviewed by (Nowacek et al., 2009b)). Successful delivery of antiretroviral drugs to the brain and purging of this viral sanctuary could effectively eliminate this form of dementia.

Our laboratory has focused its research efforts on developing long-acting parenteral drug formulations that can be maintained inside cells for extended periods and travel specifically to viral sanctuaries where ART compounds can be released. In these past studies (Dou et al., 2006; Dou et al., 2007; Dou et al., 2009; Nowacek et al., 2009b), we demonstrated that antiretroviral compounds could be manufactured into stable formulations of nanometer sized drug crystals coated in surfactant polymers, that the physical properties of these particles could be modified, and that these changes had an affect upon cellular handling. Most importantly, we demonstrated that MDM pretreated with nanoART could release drug and inhibit HIV-1 replication for up to 15 days after treatment. However, in all prior studies the effect of only one formulation was explored at a time. In the clinic, ART involves the use of multiple drugs of different classes simultaneously. We hypothesized that we could further extend the time of drug release and improve viral inhibition over our previous findings by exposing MDM to a “nanoART cocktail”. The fact that multiple formulations showed substantial improvements over a single nanoART preparation was an unexpected finding, as we believed that each would affect uptake of the others. This was not the case.

In the clinic, ART therapy commonly consists of a drug “cocktail”; this improves pharmacokinetics (PK), more effectively reduces viral loads, and decreases the risk of viral resistance (Zolopa, 2009). For example, RTV (a protease inhibitor, PI) can be used to “boost” serum levels of other PIs, such as ATV (Horberg et al., 2008). In fact, ATV is commonly prescribed in conjunction with a low dose of RTV in order to increase its serum levels (Johnson et al., 2005; Gisslen et al., 2006). A possible addition to ATV-RTV therapy is EFV, a nonnucleoside reverse transcriptase inhibitor. In 2008, the FDA recommended a combination of ATZ with RTV and EFV once daily as a possible treatment in ART-naive patients(Horberg et al., 2008).

In addition, increasing the overall drugs taken up by MDM also extended the time of drug release. A potential explanation for this finding involves intracellular drug metabolism. RTV is a very potent inhibitor of cytochrome P450 enzymes, such as CYP2B6, CYP2D6, CYP3A4/5, and others (Kumar et al., 1999; Hesse et al., 2001; Zeldin and Petruschke, 2004; Xu and Desai, 2009). In the clinic RTV is used in ART drug combinations to both increase bioavailability and reduce hepatic clearance of other antiretroviral compounds (Zeldin and Petruschke, 2004; Feldt et al., 2005; Gianotti et al., 2007; Xu and Desai, 2009). This allows for improved dosing schedules and better viral inhibition (Zeldin and Petruschke, 2004; Xu and Desai, 2009). The expression of CYP2B6, CYP2D6, and CYP3A4/5 mRNAs have been identified in alveolar macrophages suggesting that macrophages are capable of metabolizing antiretroviral medications(Anttila et al., 1997; Hukkanen et al., 1997; Raunio et al., 1999; Piipari et al., 2000; Hukkanen et al., 2002). Therefore, after nanoART are taken up by MDM, a portion of the drugs may be metabolized by the cells. By including RTV in the nanoART combination, we may be inhibiting nanoART metabolism and improving intracellular stability, thereby extending the time of drug release.

A major challenge for medicine is to improve clinical outcomes for CNS disorders related to aging, infection and degeneration. These conditions include, but are not limited to: stroke, multiple sclerosis, Parkinson's disease, Alzheimer's disease, and HAND. In all cases disease progression could be slowed, halted or potentially reversed with targeted drug delivery. Potentially useful medications exist for these diseases; unfortunately, like ART compounds, many are unable to effectively cross the BBB, enter the CNS, and potentiate a positive change(Kabanov and Gendelman, 2007; Nowacek et al., 2009a). Many neurologic diseases have an inflammatory component (Perry et al., 1995), thereby allowing immunocytes, such as macrophages, to migrate into sites of inflammation via diapedesis and chemotaxis (Kumagai et al., 1987). Therefore, we anticipate that our model of cell-mediated drug delivery of crystalline NP may be applicable to other major CNS disorders besides HAND.

This work brings us yet one step closer to realizing the use of nanoART in humans, but much work still needs to be done. In the future, we plan to elucidate mechanisms of nanoART uptake, study NP trafficking, and identify sub-cellular compartments in which nanoART are stored within MDM. In addition, we plan to investigate *in vivo* PK, biodistribution, and efficacy upon a single parenteral administration.

Supplementary Material

Refer to Web version on PubMed Central for supplementary material.

Acknowledgments

The authors thank Janice A. Taylor and James R. Talaska of the Confocal Laser Scanning Microscope Core Facility at the University of Nebraska Medical Center for providing assistance with confocal microscopy, the Nebraska Research Initiative and the Eppley Cancer Center for their support of the Core Facility. We also thank Ms. Robin Taylor for critical reading of the manuscript and outstanding graphic and literary support.

References

Anttila S, Hukkanen J, Hakkola J, Stjernvall T, Beaune P, Edwards RJ, Boobis AR, Pelkonen O, Raunio H. Expression and localization of CYP3A4 and CYP3A5 in human lung. Am J Respir Cell Mol Biol. 1997; 16:242–249. [PubMed: 9070608]

Baum MK, Rafie C, Lai S, Sales S, Page B, Campa A. Crack-cocaine use accelerates HIV disease progression in a cohort of HIV-positive drug users. J Acquir Immune Defic Syndr. 2009; 50:93–99. [PubMed: 19295339]

Best BM, Letendre SL, Brigid E, Clifford DB, Collier AC, Gelman BB, McArthur JC, McCutchan JA, Simpson DM, Ellis R, Capparelli EV, Grant I. Low atazanavir concentrations in cerebrospinal fluid. Aids. 2009; 23:83–87. [PubMed: 19050389]

Bruce RD, Altice FL, Gourevitch MN, Friedland GH. Pharmacokinetic drug interactions between opioid agonist therapy and antiretroviral medications: implications and management for clinical practice. J Acquir Immune Defic Syndr. 2006a; 41:563–572. [PubMed: 16652030]

Bruce RD, McCance-Katz E, Kharasch ED, Moody DE, Morse GD. Pharmacokinetic interactions between buprenorphine and antiretroviral medications. Clin Infect Dis. 2006b; 43(Suppl 4):S216–223. [PubMed: 17109308]

Danel C, Moh R, Chaix ML, Gabillard D, Gnokoro J, Diby CJ, Toni T, Dohoun L, Rouzioux C, Bissagnene E, Salamon R, Anglaret X. Two-months-off, four-months-on antiretroviral regimen increases the risk of resistance, compared with continuous therapy: a randomized trial involving West African adults. J Infect Dis. 2009; 199:66–76. [PubMed: 18986246]

Dou H, Grotepas CB, McMillan JM, Destache CJ, Chaubal M, Werling J, James K, Rabinow B, Gendelman HE. Macrophage Delivery of Nanoformulated Antiretroviral Drug to the Brain in a Murine Model of NeuroAIDS. J Immunol. 2009

Dou H, Morehead J, Destache CJ, Kingsley JD, Shlyakhtenko L, Zhou Y, Chaubal M, Werling J, Kipp J, Rabinow BE, Gendelman HE. Laboratory investigations for the morphologic, pharmacokinetic,

and anti-retroviral properties of indinavir nanoparticles in human monocyte-derived macrophages. Virology. 2007; 358:148–158. [PubMed: 16997345]

Dou H, Destache CJ, Morehead JR, Mosley RL, Boska MD, Kingsley J, Gorantla S, Poluektova L, Nelson JA, Chaubal M, Werling J, Kipp J, Rabinow BE, Gendelman HE. Development of a macrophage-based nanoparticle platform for antiretroviral drug delivery. Blood. 2006; 108:2827–2835. [PubMed: 16809617]

Ellis R, Langford D, Masliah E. HIV and antiretroviral therapy in the brain: neuronal injury and repair. Nat Rev Neurosci. 2007; 8:33–44. [PubMed: 17180161]

Epstein LG, Gendelman HE. Human immunodeficiency virus type 1 infection of the nervous system: pathogenetic mechanisms. Ann Neurol. 1993; 33:429–436. [PubMed: 8498818]

Feldt T, Oette M, Kroidl A, Gobels K, Leidel R, Sagir A, Kuschak D, Haussinger D. Atazanavir for treatment of HIV infection in clinical routine: efficacy, pharmacokinetics and safety. Eur J Med Res. 2005; 10:7–10. [PubMed: 15737947]

Fellay J, Boubaker K, Ledergerber B, Bernasconi E, Furrer H, Battegay M, Hirschel B, Vernazza P, Francioli P, Greub G, Flepp M, Telenti A. Prevalence of adverse events associated with potent antiretroviral treatment: Swiss HIV Cohort Study. Lancet. 2001; 358:1322–1327. [PubMed: 11684213]

Garvie PA, Lawford J, Flynn PM, Gaur AH, Belzer M, McSherry GD, Hu C. Development of a directly observed therapy adherence intervention for adolescents with human immunodeficiency virus-1: application of focus group methodology to inform design, feasibility, and acceptability. J Adolesc Health. 2009; 44:124–132. [PubMed: 19167660]

Gendelman HE, Orenstein JM, Martin MA, Ferrua C, Mitra R, Phipps T, Wahl LA, Lane HC, Fauci AS, Burke DS, et al. Efficient isolation and propagation of human immunodeficiency virus on recombinant colony-stimulating factor 1-treated monocytes. J Exp Med. 1988; 167:1428–1441. [PubMed: 3258626]

Gianotti N, Soria A, Lazzarin A. Antiviral activity and clinical efficacy of atazanavir in HIV-1-infected patients: a review. New Microbiol. 2007; 30:79–88. [PubMed: 17619250]

Gisslen M, Ahlqvist-Rastad J, Albert J, Blaxhult A, Hamberg AK, Lindback S, Sandstrom E, Uhnoo I. Antiretroviral treatment of HIV infection: Swedish recommendations 2005. Scand J Infect Dis. 2006; 38:86–103. [PubMed: 16562361]

Gray F, Adle-Biassette H, Chretien F, Lorin de la Grandmaison G, Force G, Keohane C. Neuropathology and neurodegeneration in human immunodeficiency virus infection. Pathogenesis of HIV-induced lesions of the brain, correlations with HIV-associated disorders and modifications according to treatments. Clin Neuropathol. 2001; 20:146–155. [PubMed: 11495003]

Hawkins T. Appearance-related side effects of HIV-1 treatment. AIDS Patient Care STDS. 2006; 20:6–18. [PubMed: 16426151]

Hesse LM, von Moltke LL, Shader RI, Greenblatt DJ. Ritonavir, efavirenz, and nelfinavir inhibit CYP2B6 activity in vitro: potential drug interactions with bupropion. Drug Metab Dispos. 2001; 29:100–102. [PubMed: 11159797]

Horberg M, Klein D, Hurley L, Silverberg M, Towner W, Antoniskis D, Kovach D, Mogyoros M, Blake W, Dobrinich R, Dodge W. Efficacy and safety of ritonavir-boosted and unboosted atazanavir among antiretroviral-naive patients. HIV Clin Trials. 2008; 9:367–374. [PubMed: 19203902]

Hukkanen J, Pelkonen O, Hakkola J, Raunio H. Expression and regulation of xenobiotic-metabolizing cytochrome P450 (CYP) enzymes in human lung. Crit Rev Toxicol. 2002; 32:391–411. [PubMed: 12389869]

Hukkanen J, Hakkola J, Anttila S, Piipari R, Karjalainen A, Pelkonen O, Raunio H. Detection of mRNA encoding xenobiotic-metabolizing cytochrome P450s in human bronchoalveolar macrophages and peripheral blood lymphocytes. Mol Carcinog. 1997; 20:224–230. [PubMed: 9364212]

Johnson M, Grinsztejn B, Rodriguez C, Coco J, DeJesus E, Lazzarin A, Lichtenstein K, Rightmire A, Sankoh S, Wilber R. Atazanavir plus ritonavir or saquinavir, and lopinavir/ritonavir in patients experiencing multiple virological failures. Aids. 2005; 19:685–694. [PubMed: 15821394]

Kabanov AV, Gendelman HE. Nanomedicine in the diagnosis and therapy of neurodegenerative disorders. Progress in Polymer Science. 2007; 32:1054–1082. [PubMed: 20234846]

Kalter DC, Greenhouse JJ, Orenstein JM, Schnittman SM, Gendelman HE, Meltzer MS. Epidermal Langerhans cells are not principal reservoirs of virus in HIV disease. J Immunol. 1991; 146:3396–3404. [PubMed: 2026871]

Kraft-Terry SD, Buch SJ, Fox HS, Gendelman HE. A coat of many colors: neuroimmune crosstalk in human immunodeficiency virus infection. Neuron. 2009; 64:133–145. [PubMed: 19840555]

Kumagai AK, Eisenberg JB, Pardridge WM. Absorptive-mediated endocytosis of cationized albumin and a beta-endorphin-cationized albumin chimeric peptide by isolated brain capillaries. Model system of blood-brain barrier transport. J Biol Chem. 1987; 262:15214–15219. [PubMed: 2959663]

Kumar GN, Dykstra J, Roberts EM, Jayanti VK, Hickman D, Uchic J, Yao Y, Surber B, Thomas S, Granneman GR. Potent inhibition of the cytochrome P-450 3A-mediated human liver microsomal metabolism of a novel HIV protease inhibitor by ritonavir: A positive drug-drug interaction. Drug Metab Dispos. 1999; 27:902–908. [PubMed: 10421617]

Mascolini M, Larder BA, Boucher CA, Richman DD, Mellors JW. Broad advances in understanding HIV resistance to antiretrovirals: report on the XVII International HIV Drug Resistance Workshop. Antivir Ther. 2008; 13:1097–1113. [PubMed: 19195337]

Meade CS, Hansen NB, Kochman A, Sikkema KJ. Utilization of medical treatments and adherence to antiretroviral therapy among HIV-positive adults with histories of childhood sexual abuse. AIDS Patient Care STDS. 2009; 23:259–266. [PubMed: 19260772]

Metzner KJ, Giulieri SG, Knoepfel SA, Rauch P, Burgisser P, Yerly S, Gunthard HF, Cavassini M. Minority quasispecies of drug-resistant HIV-1 that lead to early therapy failure in treatment-naive and -adherent patients. Clin Infect Dis. 2009; 48:239–247. [PubMed: 19086910]

Mosmann T. Rapid colorimetric assay for cellular growth and survival: application to proliferation and cytotoxicity assays. J Immunol Methods. 1983; 65:55–63. [PubMed: 6606682]

Murri R, Lepri AC, Cicconi P, Poggio A, Arlotti M, Tositti G, Santoro D, Soranzo ML, Rizzardini G, Colangeli V, Montroni M, Monforte AD. Is moderate HIV viremia associated with a higher risk of clinical progression in HIV-infected people treated with highly active antiretroviral therapy: evidence from the Italian cohort of antiretroviral-naive patients study. J Acquir Immune Defic Syndr. 2006; 41:23–30. [PubMed: 16340469]

Nowacek A, Gendelman HE. NanoART, neuroAIDS and CNS drug delivery. Nanomed. 2009; 4:557–574.

Nowacek A, Kosloski LM, Gendelman HE. Neurodegenerative disorders and nanoformulated drug development. Nanomed. 2009a; 4:541–555.

Nowacek AS, Miller RL, McMillan J, Kanmogne G, Kanmogne M, Mosley RL, Ma Z, Graham S, Chaubal M, Werling J, Rabinow B, Dou H, Gendelman HE. NanoART synthesis, characterization, uptake, release and toxicology for human monocyte-macrophage drug delivery. Nanomed. 2009b; 4:903–917.

Paterson DL, Swindells S, Mohr J, Brester M, Vergis EN, Squier C, Wagener MM, Singh N. Adherence to protease inhibitor therapy and outcomes in patients with HIV infection. Ann Intern Med. 2000; 133:21–30. [PubMed: 10877736]

Perry VH, Bell MD, Brown HC, Matyszak MK. Inflammation in the nervous system. Curr Opin Neurobiol. 1995; 5:636–641. [PubMed: 8580715]

Piipari R, Savela K, Nurminen T, Hukkanen J, Raunio H, Hakkola J, Mantyla T, Beaune P, Edwards RJ, Boobis AR, Anttila S. Expression of CYP1A1, CYP1B1 and CYP3A, and polycyclic aromatic hydrocarbon-DNA adduct formation in bronchoalveolar macrophages of smokers and non-smokers. Int J Cancer. 2000; 86:610–616. [PubMed: 10797280]

Raunio H, Hakkola J, Hukkanen J, Lassila A, Paivarinta K, Pelkonen O, Anttila S, Piipari R, Boobis A, Edwards RJ. Expression of xenobiotic-metabolizing CYPs in human pulmonary tissue. Exp Toxicol Pathol. 1999; 51:412–417. [PubMed: 10445407]

Royal SW, Kidder DP, Patrabansh S, Wolitski RJ, Holtgrave DR, Aidala A, Pals S, Stall R. Factors associated with adherence to highly active antiretroviral therapy in homeless or unstably housed adults living with HIV. AIDS Care. 2009; 21:448–455. [PubMed: 19401865]

Valcour V, Paul R. HIV infection and dementia in older adults. Clin Infect Dis. 2006; 42:1449–1454. [PubMed: 16619159]

Varatharajan L, Thomas SA. The transport of anti-HIV drugs across blood-CNS interfaces: summary of current knowledge and recommendations for further research. Antiviral Res. 2009; 82:A99–109. [PubMed: 19176219]

Xu L, Desai MC. Pharmacokinetic enhancers for HIV drugs. Curr Opin Investig Drugs. 2009; 10:775–786.

Zeldin RK, Petruschke RA. Pharmacological and therapeutic properties of ritonavir-boosted protease inhibitor therapy in HIV-infected patients. J Antimicrob Chemother. 2004; 53:4–9. [PubMed: 14657084]

Zolopa AR. The evolution of HIV treatment guidelines: Current state-of-the-art of ART. Antiviral Res. 2009

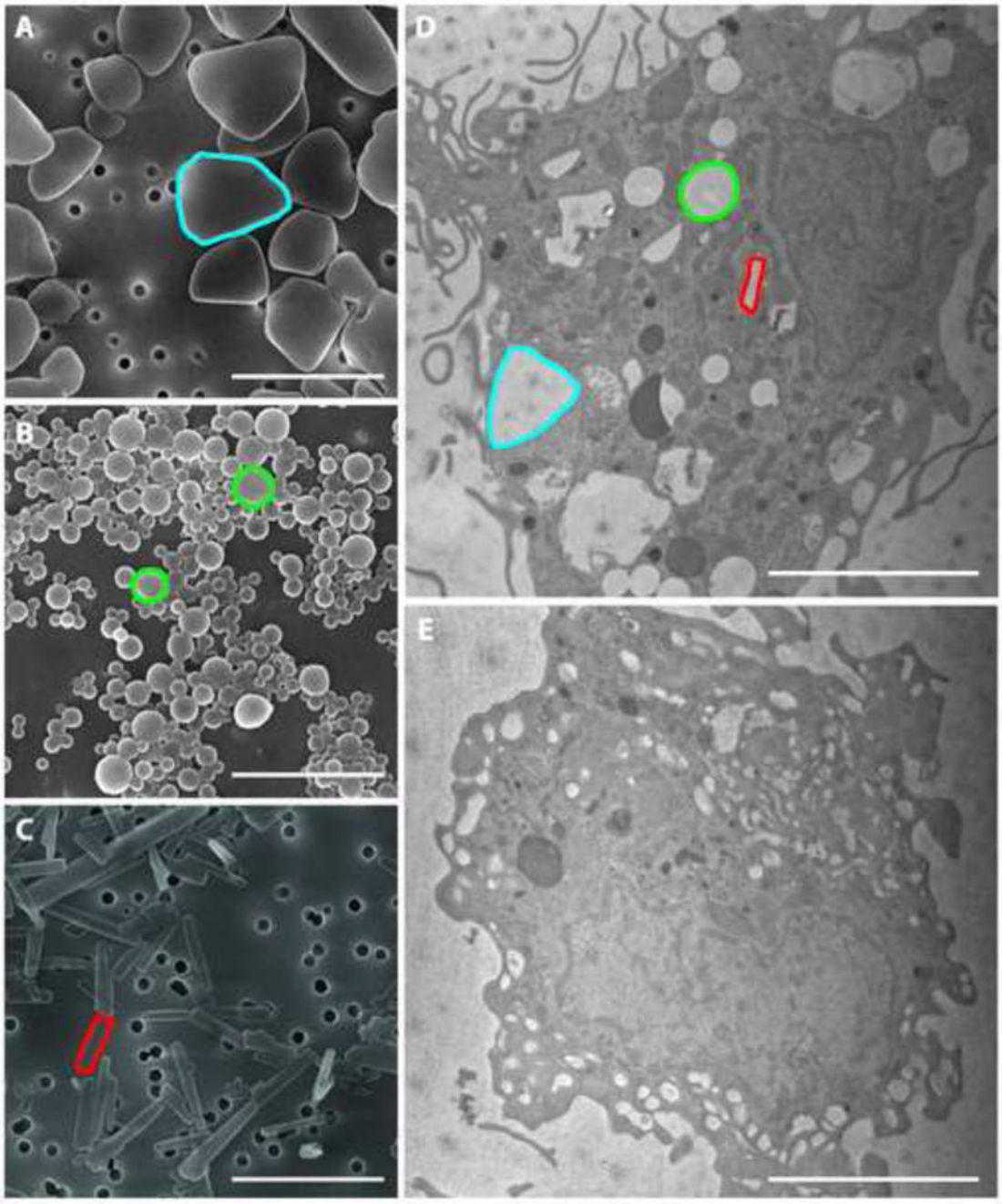

Figure 1. NanoART morphology

Scanning electron microscopy analyses (magnification 30,000x) of nanoformulations shown include ATV in blue (A), EFV in green (B), and RTV in red (C) on top of a 0.2 μm polycarbonate filtration membrane. Measure bar equals 1μm (A,B,C) and 3μm (D,E). ATV(A) showed polygonal structures with sizes of approximately 1 μm; EFV (B) showed spherical structures of approximately 300 nm; RTV (C) showed rod structures with sizes of approximately 1 μm. Transmission electron microscope (magnification, 15,000x) demonstrated uptake of nanoART into MDMs exposed to a combination of ATV, EFV and RTV (D) compared to untreated cells (E). Within the cell, each type of nanoART is readily

identifiable by its unique shape and an example has been outlined in blue (ATV), green (EFV), and red (RTV).

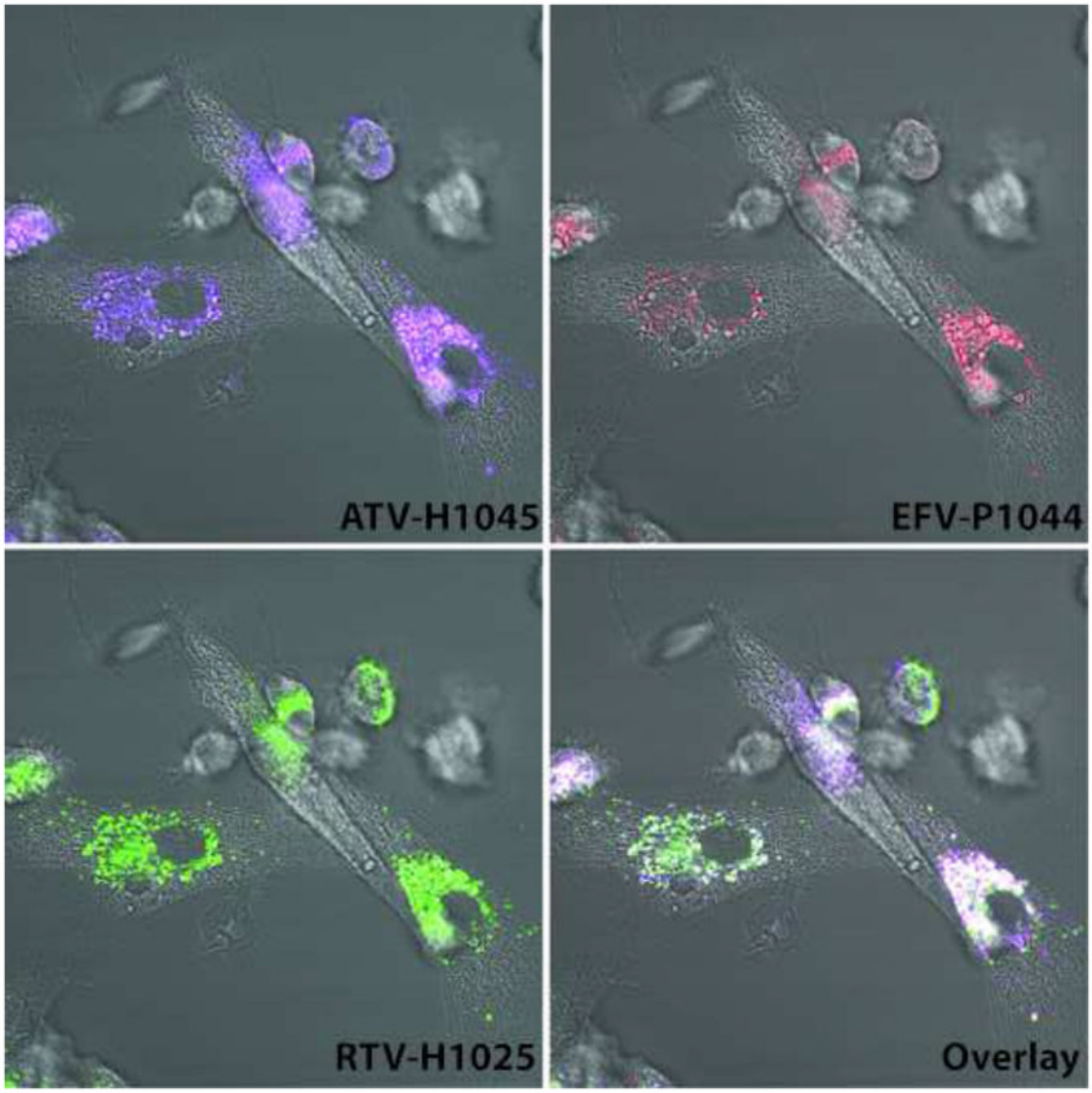

Figure 2. Simultaneous MDM uptake of nanoformulated ATV, RTV, and EFV

Fluorescence microscopy of MDM incubated with 100 μM each of ATV-H1045 (purple) labeled with Vybrant DiO cell-labeling solution, RTV-H1025 (green) labeled with Vybrant DiD cell-labeling solution, and EFV-P1044 (red) with rhodamine B 1,2-dihexadecanoyl-sn-glycero-3-phospho-ethanolamine, triethylammonium salt. Overlay (white) represents colocalization of all three nanoART to cytoplasmic vesicles. Images were acquired after 2 h of incubation with nanoART combination.

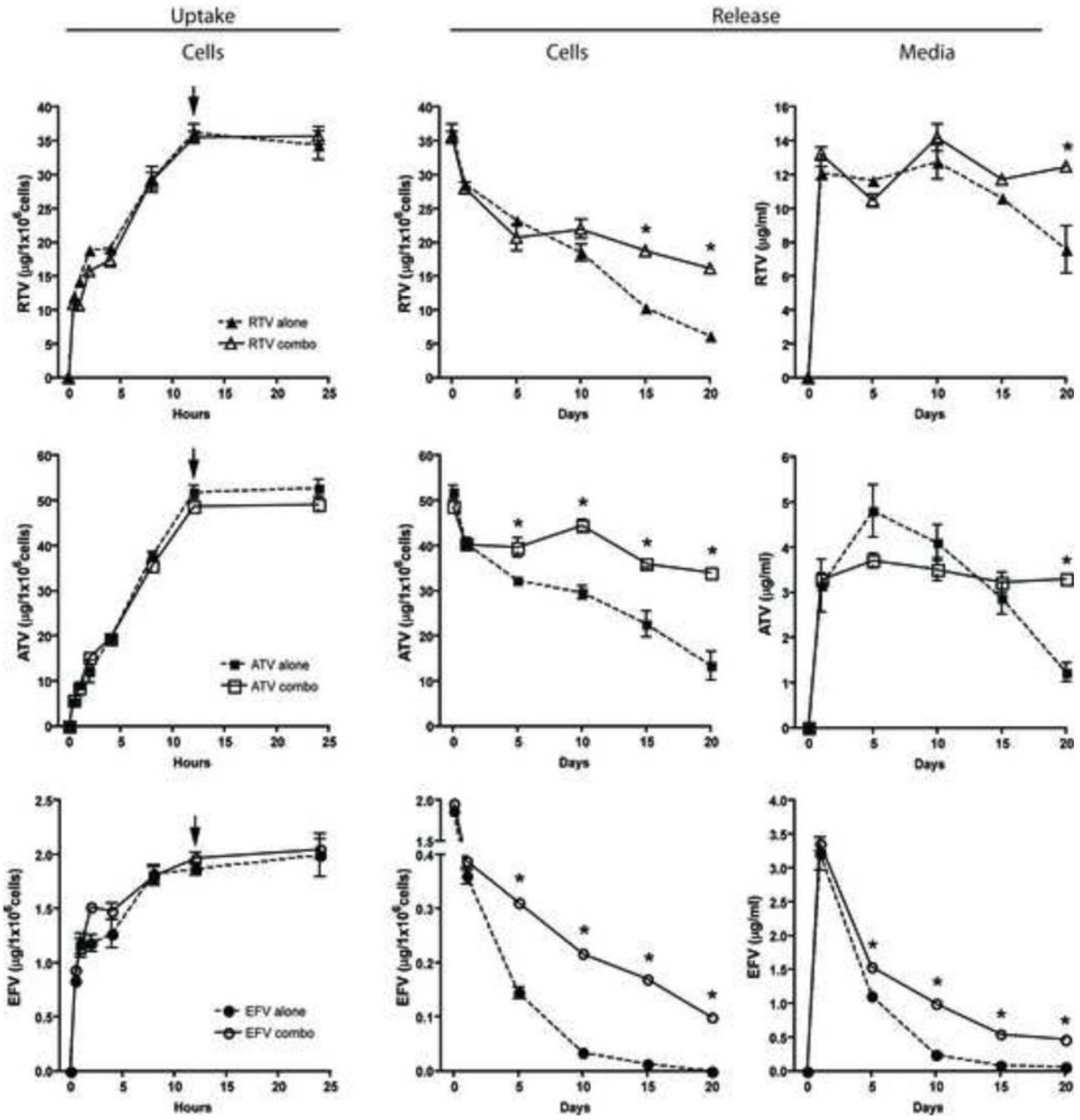

Figure 3. MDM uptake and release of nanoformulated RTV, ATV, and EFV

Uptake: Levels of RTV-H1025, ATV-H1045, and EFV-P1044 in cell lysates of cultured MDM treated with 100 μM of each nanoART alone or in combination (nanoART*) and collected at specified times were determined by HPLC. Arrows indicate initiation time for release studies. Release: Levels of RTV, ATV, and EFV were determined over 20 days by HPLC in both cell lysates (cells) and extracellular media (media) at specified times. Data represent mean ± SD for n = 3 determinations/time point. Asterisks indicate significant differences ($p < 0.05$) between levels of drug when cells were treated with one nanoART compared to a combination of all three.

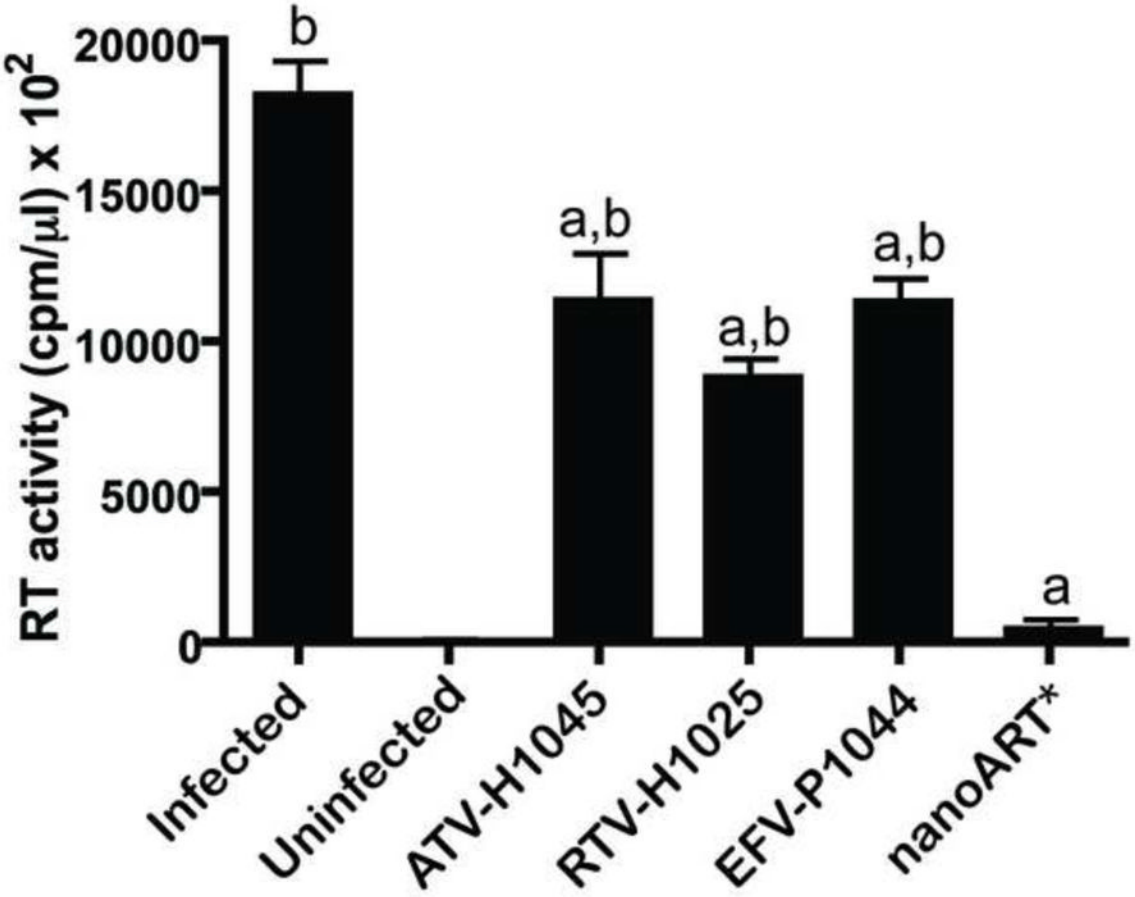

Figure 4. Antiretroviral activities for nanoART

Comparison of antiretroviral effects of ATV-H1045, RTV-H1025, and EFV-P1044 alone or in combination (nanoART*) 20 days after pretreatment with nanoART as measured by RT activity. RT activities were measured by ^{3}H-TTP incorporation. Data represent mean ± SD for n = 6 determinations/treatment. “a” indicates significant difference ($p< 0.001$) from no nanoART treatment (Infected). “b” indicates significant difference ($p< 0.001$) from nanoART*.

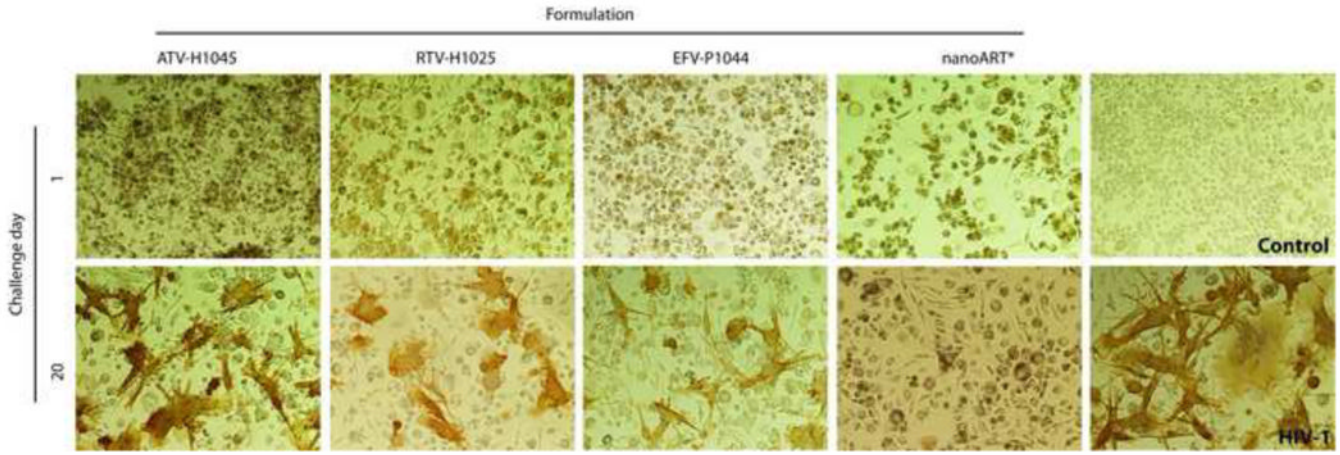

Figure 5. NanoART effects HIV-1 p24 antigen expression in virus-infected MDM

Comparison of antiretroviral effects of ATV-H1045, RTV-H1025, and EFV-P1044 alone or combination (nanoART*) over 20 days in MDM pretreated with nanoART. Ten days after each viral challenge cells were immunostained for HIV-1 p24 antigen (brown). Images (40x) are representative of n = 6 determinations/time point. Cells treated with ATV-H1045, RTV-H1025, or EFV-P1044 alone showed decrease of antiretroviral protection and increased HIV p24 expression at 20 days; while cells treated with a combination of all three nanoART maintained complete suppression of viral p24 production.

Table 1

Physicochemical characteristics of nanoformulated ART drugs.

Name	Drug	Surfactants	Size (nm)	Charge (mV)
ATV-H1045	ATV	P188, $mPEG_{2000}$-DSPE, DOTAP	645	14.5
EFV-P1044	EFV	PLGA, PVA, CTAB	300	7.4
RTV-H1025	RTV	P188, $mPEG_{2000}$-DSPE, DOTAP	620	15.5